

Restore from Restored: Single Image Denoising with Pseudo Clean Image

Seunghwan Lee¹, Donghyeon Cho², Jiwon Kim³, and Tae Hyun Kim¹

¹ Department of Computer Science, Hanyang University, Seoul, Korea
seunghwanlee@hanyang.ac.kr, lliger9@gmail.com

² Department of Electronic Engineering, Chungnam National University, Daejeon, Korea

cdh12242@gmail.com

³ SK T-Brain, Seoul, Korea
jk@sktbrain.com

Abstract. Under certain statistical assumptions of noise (e.g., zero-mean noise), recent self-supervised approaches for denoising have been introduced to learn network parameters without ground-truth clean images, and these methods can restore an image by exploiting information available from the given input (i.e., internal statistics) at test time. However, self-supervised methods are not yet properly combined with conventional supervised denoising methods which train the denoising networks with a large number of external training images. Thus, we propose a new denoising approach that can greatly outperform the state-of-the-art supervised denoising methods by adapting (fine-tuning) their network parameters to the given specific input through self-supervision without changing the fully original network architectures. We demonstrate that the proposed method can be easily employed with state-of-the-art denoising networks without additional parameters, and achieve state-of-the-art performance on numerous denoising benchmark datasets.

Keywords: Single image denoising, Deep neural network, Fine-tuning, Self-supervision, Internal statistics

1 Introduction

When a scene is captured by an imaging device, a desired clean image \mathbf{X} is corrupted by noise \mathbf{n} . We usually assume that the noise \mathbf{n} is an Additive White Gaussian Noise (AWGN), and the observed noisy image \mathbf{Y} can be expressed as $\mathbf{Y} = \mathbf{X} + \mathbf{n}$. In particular, noise \mathbf{n} increases in environments with high ISO, short exposure times, and low-light conditions. Image denoising is a task that restores the clean image \mathbf{X} by removing noise \mathbf{n} from the noisy input \mathbf{Y} , and is a highly ill-posed problem. Thus, substantial literature concerning denoising problem has been introduced [16,27,8,24,10,13,25,6].

Recent deep learning technologies have been used not only to obtain an image prior model via discriminative learning but also to design feed-forward denoising

networks that directly produce denoised clean outputs. These methods train networks for denoising in a supervised manner by using pairs of input images and ground-truth clean images (noise-to-truth), and have shown satisfactory results. However, supervised methods are limited in performance when the noise distribution of the test image is considerably different from the distribution of noise in the training dataset, i.e., when domain misalignment occurs. To overcome these issues, researchers have proposed self-supervised training methods recently, such as noise-to-noise [21], noise-to-void [19], and noise-to-self [5], which allow to train the denoising networks without using the ground-truth clean images. These methods are based on statistical assumptions, such as zero-mean noise (i.e., $\mathbb{E}(\mathbf{n}) = 0$), and specialized for dealing with unknown noise whose distribution is not common. However, self-supervised approaches have limitations in removing noise with known distribution (e.g., Gaussian noise) and do not show satisfactory results over supervision-based denoising methods.

In this study, we aim to remove noise from known distribution (e.g., Gaussian noise), and improve the performance of existing supervision-based networks through a method that updates the network parameters adaptively using the information available from the given noisy input image at test-time. First, we start with a fully pre-trained network in a supervised manner to fully explore the large external database. Then, the network is fine-tuned using our proposed loss function which can overcome the limitations of conventional self-supervised methods (i.e., noise-to-void [19], noise-to-self [5]) during the inference phase. Based on theoretical basis, we can efficiently improve the denoising performance by exploiting the self-similarity present in the input image. Self-similarity is a property that a large number of corresponding patches are existing within a single image (patch-recurrence), and it has been employed in numerous super-resolution tasks to enhance the restoration quality [15,28,18].

We experimentally show that the adaptation via self-supervision during the inference stage can consistently increase denoising performance regardless of test dataset and the deep learning architectures if they are fully convolutional networks (FCNs). Overall, our method obtains generalization based on supervised methods by using the large external training data while breaking the limit of previously achieved performance through adoption of the self-supervised approaches.

In this study, we present a new and efficient fine-tuning method which allows to train the denoising networks by supervision and self-supervision. The contributions of this paper are summarized as follows:

- We present a new learning algorithm, which allows to utilize the internal statistics of a natural image (i.e., self-similarity, patch-recurrence) very efficiently.
- Our proposed algorithm can be easily applied to many conventional denoising networks without modifying the network architectures.
- We demonstrate conventional supervised denoising networks can be fine-tuned by self-supervised learning techniques for a given specific test input

and improve performance by a large margin in removing noise with known distribution (e.g., Gaussian).

2 Related Work

In this section, we review numerous denoising methods with and without the use of ground-truth clean images for training.

Image denoising is an actively studied area in image processing, and various denoising methods have been introduced, such as self-similarity-based methods [7,9,14], sparse-representation-based methods [26,11], and external database exploiting methods [4,3,23,30]. With the recent development of deep learning technologies, the denoising technique has been also improved, and remarkable progress has been achieved in this field. Specifically, after Xie *et al.* [29] adopted deep neural networks for denoising and inpainting tasks, numerous follow-up studies have been proposed [31,32,33,35,20,22,34,17,2].

Based on deep convolutional neural network (CNN), Zhang *et al.* [31] proposed a deep network to learn a residual image with a skip connection between the input and output of the network, and accelerated training speed and enhanced denoising performance. Zhang *et al.* [32] also proposed IRCNN to train a Gaussian denoiser and this network can be combined with conventional model-based optimization methods to solve various image restoration problems such as denoising, super-resolution, and deblurring. Furthermore, Zhang *et al.* [33] proposed a fast and efficient denoising network FFDNet, which takes cropped sub-images and a noise level map as inputs. In addition to being fast, FFDNet can handle locally varying and a wide range of noise levels. Zhang *et al.* [35] introduced a very deep residual dense network (RDN) which is composed of multiple residual dense blocks. RDN achieves superior performance by exploiting all the hierarchical local and global features through densely connected convolutional layers and dense feature fusion. To incorporate long-range dependencies among pixels, Zhang *et al.* [34] proposed a residual non-local attention network (RNAN), which consists of a trunk and (non-) local mask branches. In [22], the non-local block was used with a recurrent mechanism to increase the receptive field of the denoising network. Recently, CBDNet [17] and RIDNet [2] were introduced to handle noise in real photographs where the noise level is unknown (blind denoising). CBDNet is a two-step approach that combines noise estimation and non-blind denoising tasks, whereas RIDNet is a single-stage method that employs feature attention.

After deep CNN was adopted to increase denoising performance, various research directions, such as residual learning for constructing deeper networks, non-local or hierarchical features for enlarging the receptive fields, and noise level estimation for real photographs, have been considered. However, such works remain limited to the cases in which networks are supervised by true clean images (noise-to-truth). Recently, several self-supervision-based studies have been conducted to leverage only noisy images for network training without true clean images, which is crucial to handle noise with unknown distribution. Lehtinen *et*

al. [21] demonstrated that a denoising network can be trained without clean images. The network was trained with pairs of noisy patches (noise-to-noise) based on statistical reasoning that the expectation of randomly corrupted signal is close to the clean target data. Furthermore, to avoid constructing pairs of noisy images, Krull *et al.* [19] proposed a noise-to-void method and introduced a blind-spot network. Specifically, only the center pixel of the input patch was considered in the loss function, and the network was trained to predict its center pixel without any true clean dataset. Similarly, Baston and Royer [5] introduced a noise-to-self method for training the network without knowing the ground-truth data.

However, these self-supervision-based methods cannot outperform supervised methods where the distribution of the input is identical to training sample distribution. In this work, we focus on dealing with noise with known distribution (e.g., Gaussian), and enhance the denoising quality by adapting the parameter of the network trained in a supervised manner. Specifically, we use the supervised approach (i.e., noise-to-truth) during the training phase to achieve state-of-the-art performance by generalization, and use a proposed self-supervision-based learning algorithm on the test input image during the inference stage to further improve the denoising performance by parameter adaptation. In the end, our supervised network can be adapted to a specific input image during the inference phase based on the self-supervision with only few gradient update steps.

The proposed method can achieve state-of-the-art performance by not only exploring the large external datasets, but also exploiting internal information available from the given input image, such as self-similarity as in [5,19,28].

3 Supervision vs. Self-supervision for Image Denoising

Natural images have patches that are redundant (i.e., self-similarity) within the images [15,18,28], and we can remove zero-mean random noise \mathbf{n} in the given input image by using these similar, but differently corrupted patches [36]. However, conventional supervised denoising networks trained using a large external dataset cannot exploit patch-recurrence in the given input image due to the limited capacity of the network architectures (e.g., receptive field), and thus, the performance is limited.

To alleviate this problem, recent denoising networks employ non-local operation modules to exploit self-similarity [20,22]. Nevertheless, they are still limited and restrict search range of the non-local operation module due to network size and inference speed. That is, current supervised methods cannot fully utilize recurring patches which are far away from each other (e.g., more than several hundred pixels away) within a single image.

3.1 Noise-to-void and noise-to-self training

Recent self-supervision-based single image denoising methods (i.e., noise-to-void [19], noise-to-self [5]) which attempt to train the networks without using the ground-

truth images can effectively exploit self-similarity by minimizing specially designed loss functions at test-time. These self-supervision-based methods can efficiently remove unknown noise (i.e., corrupted by unknown distribution) by utilizing similar patches in the given test image, whereas conventional supervised methods cannot handle this unexpected noise. Specifically, the dedicated loss function in [19,5], which takes two noisy patches as input is given by,

$$Loss(\theta) = \sum_i (\mathbf{f}_\theta(\mathbf{B}(\mathbf{y}_i)) - \mathbf{y}_i)^2, \quad (1)$$

where a function \mathbf{f} denotes a fully convolutional neural network (FCN), and the parameter of the FCN is θ . Input noisy patch centered at a pixel location i is given as \mathbf{y}_i . In particular, a blind-spot function \mathbf{B} removes color value of the center pixel of a patch \mathbf{y}_i , and fills that pixel with one of color values from neighboring pixels (refer to [19] for details). In this formulation, specially designed function \mathbf{B} plays a key role not to learn an identity mapping but to learn denoising ability by optimizing (1).

Under two assumptions that the ground-truth center pixel value and the expectation of the copied neighboring pixel value are equal, and the given M patches $\{\mathbf{y}_1, \dots, \mathbf{y}_M\}$ are well aligned (i.e., M corresponding patches), we can learn an optimal parameter $\theta^\#$ by optimizing the loss function in (1). The learned network $\mathbf{f}_{\theta^\#}^\#$ will predict a latent patch which is an averaged version of the corresponding input patches $\frac{1}{M} \sum_{m=1}^M \mathbf{y}_m$, and the noise variance becomes $\frac{1}{M} \sigma^2$ where σ denotes the standard deviation of the noise \mathbf{n} in the input patches. However, due to the blind-spot function \mathbf{B} , training the network is difficult and tricky. Moreover, it takes much time because the training process requires large patch but to calculate the gradients for only a single output pixel (i.e., center pixel).

	pre-trained [31]	fine-tuned by noise-to-void [19]	fine-tuned by ours
PSNR (dB) ($\sigma = 10$)	35.85	35.72	35.99
PSNR (dB) ($\sigma = 40$)	29.07	29.03	29.31

Table 1. Fine-tuning results by [19] from the pre-trained baseline model DnCNN [31]. Input images from Urban100 dataset are corrupted by random Gaussian noise with different standard deviations ($\sigma = 10, 40$).

Although self-supervision-based methods can deal with unknown noise, it is not easy to outperform the conventional supervision-based methods when

the noisy input image is corrupted by learned and known noise distribution. For example, in the work of Ehret et al. [12], proposed self-supervised video denoising network is fine-tuned from a fully pre-trained model with Gaussian noise which can remove unknown noise very effectively. However, this fine-tuned model cannot surpass its pre-trained initial network (baseline) when the input is corrupted by Gaussian noise as reported in [12]. Similarly, in Table 1, we compare the performance of noise-to-void method [19] before and after fine-tuning with self-supervision. A fully pre-trained Gaussian denoiser (DnCNN [31]) is used as initial network (baseline) of the method, and then fine-tuned according to steps in [19]. Unfortunately, we can see performance drop ($\approx 0.1\text{dB}$) of self-supervised approach [31] after fine-tuning when the test image is corrupted by Gaussian noise.

Therefore, unlike previous self-supervision-based methods which attempt to handle unknown noise, we aim to remove noise from known distribution (e.g., Gaussian noise) based on self-supervision while overcoming their limitations in this study as shown in Table 1.

4 Restoration from restored image

In this section, we present a novel denoiser that improves restoration performance by deriving the benefits of a large external training dataset, and self-similarity from an input test image. Such benefits are derived by integrating both supervised and self-supervised methods.

4.1 Restore-from-restored

To solve the problem of self-supervised learning methods in removing noise from pre-trained distribution, we introduce a self-supervision-based fine-tuning algorithm, which is easy to train, and more, outperforms the pre-trained model and shows state-of-the-art denoising performance after fine-tuning.

The key idea of the proposed method is using pairs of rendered *images* for training rather than using pairs of noisy *patches* as used in the loss function (1). The proposed loss function to fine-tune the fully pre-trained network parameter θ_0 is given by,

$$Loss(\theta) = \sum_{j=1}^N (\mathbf{f}_{\theta}(\mathbf{f}_{\theta_0}(\mathbf{Y}) + \mathbf{n}_j) - \mathbf{f}_{\theta_0}(\mathbf{Y}))^2, \quad (2)$$

where N denotes the number of train dataset for fine-tuning and \mathbf{n}_j is a random zero-mean Gaussian noise whose standard deviation is σ .

Note that, unlike previous patch-based loss function in (1), the proposed loss function takes images \mathbf{Y} as input and does not use the troublesome blind-spot function \mathbf{B} . Furthermore, as our training set is composed of initially restored frame $\mathbf{f}_{\theta_0}(\mathbf{Y})$ and its noisy version, we can easily generate pairs of training images as many as possible from a given test image. Therefore, we can train the network without using the ground-truth image (i.e., self-supervision method) but using

the pseudo clean target $\mathbf{f}_{\theta_0}(\mathbf{Y})$, and minimize the proposed loss function more easily than noise-to-void/noise-to-self training algorithm since it can be trained in image-by-image manner. As the proposed model can be trained from restored image and its noisy version, the proposed training algorithm is dubbed “*restore-from-restoration*”.

By optimizing the proposed loss function in (2), we can fine-tune and estimate an optimal network parameter θ^* which minimizes the distance between $\mathbf{f}_{\theta}(\mathbf{f}_{\theta_0}(\mathbf{Y}) + \mathbf{n})$ and $\mathbf{f}_{\theta_0}(\mathbf{Y})$. The optimal parameter θ^* can yield a latent image $\mathbf{f}_{\theta^*}(\mathbf{Y})$, which is $\frac{1}{N} \sum_{j=1}^N (\mathbf{f}_{\theta_0}(\mathbf{Y}) + \mathbf{n}_j)$. If residual noise in the initially restored image $\mathbf{f}_{\theta_0}(\mathbf{Y})$ is also an independent and identically distributed (i.i.d) zero-mean random noise, noise variance in the latent image $\mathbf{f}_{\theta^*}(\mathbf{Y})$ becomes $\sigma_{\theta_0}^2 + \frac{1}{N}\sigma^2$ where σ_{θ_0} denotes the standard deviation of the remaining noise in the image $\mathbf{f}_{\theta_0}(\mathbf{Y})$. When N approaches to infinity (recall that it’s easy to generate large number of training samples), it is natural that the expectation of the latent image $\mathbf{f}_{\theta^*}(\mathbf{Y})$ becomes $\mathbf{f}_{\theta_0}(\mathbf{Y})$ and its noise variance comes to σ_{θ_0} . The final latent frame $\mathbf{f}_{\theta^*}(\mathbf{Y})$ is the initially restored image itself, and nothing changes. However, the result can be changed when corresponding patches exist within the given specific image. Let’s assume that there are M corresponding patches $\{\mathbf{y}_1, \dots, \mathbf{y}_M\}$ in the given image \mathbf{Y} , and $N \rightarrow \infty$. Then, the expectation of the latent patch (not image) by the parameter θ^* becomes $\frac{1}{M} \sum_{j=1}^M \mathbf{f}_{\theta_0}(\mathbf{y}_j)$ and the noise variance is reduced to $\frac{1}{M}\sigma_{\theta_0}$. In general, as the residual noise level in the initially restored image is very small (i.e., $\sigma_{\theta_0} \approx 0$), the noise in the latent patch from parameter θ^* becomes negligible when M is large. Therefore, when we restore the input image \mathbf{Y} using the proposed loss function, we can expect non-uniform and spatially varying restoration quality. For example, regions where repetitive patterns exist can be restored better by fine-tuned parameter θ^* than the region restored by initial parameter θ_0 . On the other hand, a region where repetitive patterns does not exist will show similar restoration results by θ^* and θ_0 . That is, rich patch-recurrence and self-similarity in the given image can lead our fine-tuning process to success.

In addition to this conclusion, there are something more to present in this work. First, when we use an FCN as the initial baseline model \mathbf{f}_{θ_0} , we don’t need to explicitly find corresponding patches within the input image for alignment due to the translation-invariant nature of the FCN. Thus, we can still train and fine-tune the network using the full-size images to use self-similarity, and the FCN utilizes the corresponding patches from the given input image directly without any patch alignment step, which is a big advantage over previous self-supervised works [5,19]. Second, our training algorithm does not need to modify the architecture of the pre-trained model which allows us to use publicly available fully trained networks as baseline which can greatly reduce our burden for pre-training. Finally, if the residual noise in the latent frame is a zero-mean random noise, we can use L1 or L0 losses depending on the noise property of the input as introduced in [21,12,19,5].

To sum up, we present a new denoising network that can integrate the state-of-the-art supervised and self-supervised methods into a single combined net-

work, and allow to utilize the power of deep learning with a large external database and internal statistics of the input test image. In Table 2, we summarize differences between our restore-from-restored algorithm and noise-to-void (or noise-to-self) algorithms.

Self-supervised method	$E[y] \ (N \rightarrow \infty)$	$\text{Var}[y]$	Training difficulty	Unknown noise handling
Noise-to-void [19] Noise-to-self [5]	$\frac{1}{M} \sum_{j=1}^M \mathbf{y}_j$	$\frac{1}{M} \sigma^2$	High (patch-wise)	O
Restore-from-restored	$\frac{1}{M} \sum_{j=1}^M \mathbf{f}_{\theta_0}(\mathbf{y}_j)$	$\frac{1}{M} \sigma_{\theta_0}^2$	Low (image-wise)	X

Table 2. Statistics of a latent patch \mathbf{y} with the existence of M corresponding patches $\{\mathbf{y}_1, \dots, \mathbf{y}_M\}$. Note that, as $\sigma_{\theta_0} \ll \sigma$, the noise level of the latent patch by our method is much lower than the results by noise-to-void [19] and noise-to-noise [5]. Moreover, proposed method also has another advantage in the easiness of training, but cannot handle unknown noise. Note that, if $M=1$, then ours can yield result similar to the results by the pre-trained model.

Algorithm 1: *Restore-from-restored algorithm*

Input: noisy input image \mathbf{Y}

Output: fine-tuned parameter θ^* , restored image $\mathbf{f}_{\theta^*}(\mathbf{Y})$

Require: pre-trained network \mathbf{f}_{θ_0} , number of training set N , learning rate α , noise level σ

1 $i \leftarrow 0$

while $i < N$ **do**

2 $\mathbf{n} \sim \mathcal{N}(0, \sigma^2)$ // generate random noise

3 $Loss(\theta_i) = (\mathbf{f}_{\theta_i}(\mathbf{f}_{\theta_0}(\mathbf{Y}) + \mathbf{n}_i) - \mathbf{f}_{\theta_0}(\mathbf{Y}))^2$ // calculate the loss

4 $\theta_{i+1} \leftarrow \theta_i - \alpha \nabla_{\theta_i} Loss(\theta_i)$ // update the network parameter

5 $i \leftarrow i+1$

end

6 $\theta^* \leftarrow \theta_N$

Return: $\theta^*, \mathbf{f}_{\theta^*}(\mathbf{Y})$

4.2 Overall flow

Overall sketch of the proposed restore-from-restored algorithm is given in Algorithm. 1.

First, we remove the noise from the given input image using initial network parameter θ_0 , Second, we collect a single train dataset with a pair of images which consist of an initial network output $\mathbf{f}_{\theta_0}(\mathbf{Y})$ and its corrupted version with random noise. Next, using the training set, we fine-tune the network parameter. For training, we can use conventional optimization methods such as SGD and Adam for parameter update. We repeat this iterative optimization procedures several times ($=N$), and render the final clean latent image $\mathbf{f}_{\theta^*}(\mathbf{Y})$.

5 Experiments

5.1 Implementation details

In our experiments, we evaluate the proposed training algorithm based on different state-of-the-art denoising networks such as DnCNN [31], RIDNet [2], and RDN [35].

We first pre-train these denoisers with Gaussian random noise (σ is randomly selected from $[0, 50]$) on DIV2K training set with an NVIDIA 2080Ti graphic processing unit. During pre-training phase, we minimize the L1 loss between the ground-truth clean images and the network outputs with Adam, and conventional data augmentation techniques are applied (e.g., flip, flop, and rotation). These pre-trained networks are used as baseline models in our all experiments.

Note that RDN [35] shows the best performance on public benchmark site [1] in removing Gaussian noise, and recent RIDNet [2] shows competitive results. We use the light version of RDN ($D = 10$, $C = 4$, $G = 16$; refer to [35] for details) due to the limited capacity of our graphics unit (recall that we use the full-size image for utilizing self-similarity (i.e., internal statistics)).

For fine-tuning with the proposed method in Algorithm 1, we use the ADAM optimizer (learning rate = $1e-5$).

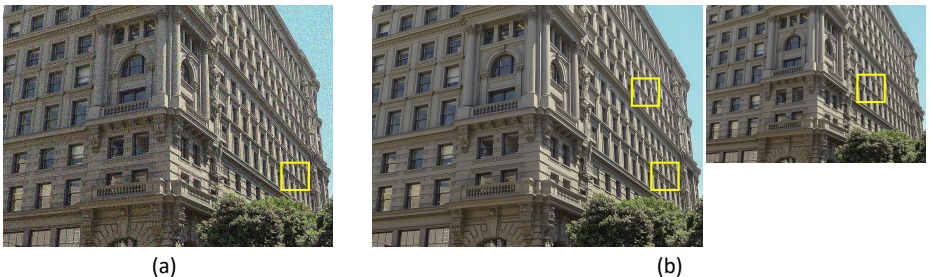


Fig. 1. (a) Noisy input image. (b) Pseudo clean images at different image scales. Note that yellow patches in (a) and (b) are corresponding to each other. Thus, pseudo clean patches at different image scales in (b) can be used to remove the noise of the yellow patch in (a).

5.2 Ablation study

In Figure 1, we show a noisy input image and its pseudo clean images at different image scales. These pseudo images can be obtained by resizing $\mathbf{f}_{\theta_0}(\mathbf{Y})$ from the pre-trained DnCNN [31]. As yellow patches in Figure 1(a)-(b) are corresponding to each other, pseudo clean patches at different image scales in Figure 1(b) can be used to remove the noise of the yellow patch in Figure 1(a).

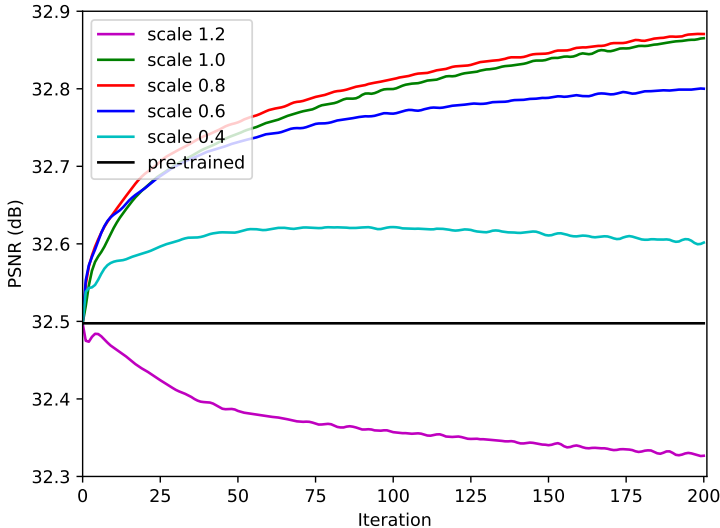


Fig. 2. Denoising results on Urban100 dataset (Gaussian noise with $\sigma = 20$) by fine-tuning DnCNN [31] with the restore-from-restored algorithm. Performance is evaluated with different sizes of pseudo clean images.

To verify this property, we fine-tune the DnCNN [31] for 200 iterations ($=N$) on the Urban100 dataset corrupted by Gaussian random noise ($\sigma = 20$). For the updates, we resize the pseudo clean image $\mathbf{f}_{\theta_0}(\mathbf{Y})$ with different scaling factors from 0.4 to 1.2. At each update, we measure the average PSNR values, and the results are shown in Figure 2. As we expect, PSNR values rise as N increases at different image scales since similar patches are existing across different image scales, as shown in Figure 1. Interestingly, when $N < 200$, we can achieve the best performance when the scaling factor is 0.8 (not 1.0), and a proper explanation on this result is the reduced noise level σ_{θ_0} by resizing. Thus, we carry out remaining experiments with the fixed scaling factor 0.8.

Next, we fine-tune the network parameter of DnCNN [31] for long iterations ($N = 1000$), and show the changes of PSNR values in Fig. 3. Pre-trained network is fine-tuned on the DIV2K testset corrupted by a Gaussian random noise ($\sigma = 40$). Notably, the black solid line denotes the the average PSNR value of

the initial network \mathbf{f}_{θ_0} . We employ the algorithm in Algorithm 1 with L1 and L2 losses. Although PSNR value by minimizing the L1 loss drops for the first few iterations, we can elevate the performance of the network up to approximately 0.15dB through 1000 updates without using the ground truth image. In the result, both PSNR values for L1 and L2 losses go up as iteration number increases, and we can see slightly better results from the L2 loss minimization (≈ 0.2 dB).

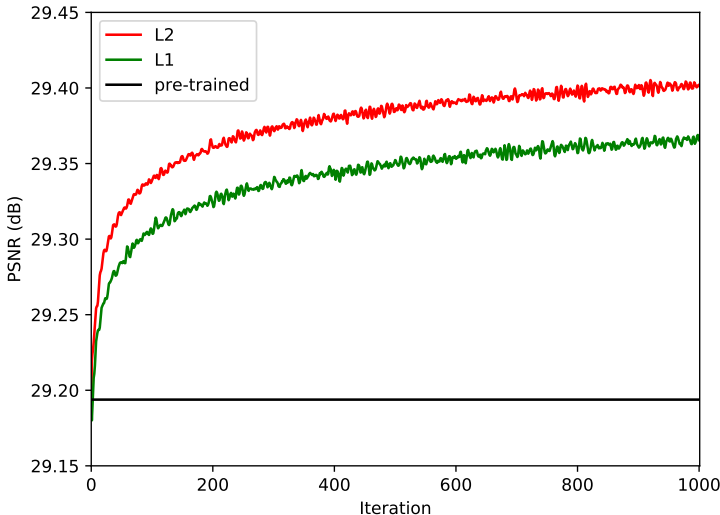


Fig. 3. Changes of average PSNR values by proposed fine-tuning. Pre-trained DnCNN [31] is fine-tuned on DIV2K testset. L1 and L2 losses are minimized for 1000 iterations ($=N$) to remove a Gaussian random noise ($\sigma = 40$). Note that black sold line denotes the average PSNR values on DIV2K testset using the pre-trained DnCNN before parameter update.

Patch-recurrence and denoising results To see whether patch-recurrence (self-similarity) really affects the denoising results, we conduct several experiments.

First, we fine-tune DnCNN [31] ($N=200$) on the BSD68 and Urban100 datasets, and the DIV2K testset. After 200 iterations, we measure the performance gain after fine-tuning, and the results are given in Table 3. We can see consistent improvements on all testsets. In particular, the PSNR gain on the Urban100 dataset is huge since many urban images include lots of repetitive patterns and recurring patches from man-made structures.

Second, we fine-tune DnCNN[31] on the Urban100 dataset, while updating the parameters with different sizes of images. To be specific, we collect 64×64 and

128×128 images cropped from the Urban100 dataset. We first collect 128×128 images by cropping the original images, and then acquire 64×64 smaller images by cropping the 128×128 images again. We compare the PSNR values after fine-tuning in Table 4. For comparison, we measure the PSNR values on small (64×64) and large (128×128) images are overlapping. We can see that the network fine-tuned with larger images renders better results on various Gaussian noise levels because larger images are likely to include more corresponding patches (i.e., large M).

In this ablation study, we verify that our algorithm can exploit self-similarity within the given input image, and thus the proposed method can produce better results where N and M are large.

	Urban100	DIV2K testset	BSD68
PSNR gain ($\sigma = 40$)	0.43	0.20	0.14

Table 3. PSNR gains before and after fine-tuning. Pre-trained DnCNN [31] is used as the baseline model, and is fine-tuned ($N = 200$). PSNR gains on Urban100, BSD68, and DIV2K testset are measured, and we can see consistent improvements on all datasets by fine-tuning.

	$\sigma = 10$	$\sigma = 20$	$\sigma = 30$	$\sigma = 40$
Small image	36.61	32.97	30.46	29.56
Large image	36.62	33.01	30.51	29.64

Table 4. Performance comparison by fine-tuning DnCNN [31] using images with different sizes. Parameters trained with large images yield consistently better results due to more corresponding patches (i.e., large M).

5.3 Quantitative and qualitative denoising results

Quantitative comparisons Results with known noise level In Table 5, we provide quantitative denoising results. DnCNN [31], RIDNet [2], and RDN [35] are fine-tuned by the proposed algorithm, and the fine-tuning results are evaluated in terms of PSNR on Urban100 and BSD68 datasets and DIV2K testset. Note that we use cropped images (500×500) for RDN [35] due to limited memory size of our graphics unit.

The performances are measured with different iteration numbers ($N=5, 10, 15, 20$), and compared with results by their baseline (fully pre-trained) versions and conventional methods (BM3D [9] and FFDNet [33]). Our fine-tuned denoisers can adapt their parameters to the specific input and produce consistently

Method	Dataset	Urban100				DIV2K testset				BSD68			
	Adaptation \ Noise	$\sigma = 10$	$\sigma = 20$	$\sigma = 30$	$\sigma = 40$	$\sigma = 10$	$\sigma = 20$	$\sigma = 30$	$\sigma = 40$	$\sigma = 10$	$\sigma = 20$	$\sigma = 30$	$\sigma = 40$
BM3D [9]	-	35.77	31.92	29.38	27.06	36.15	32.13	29.58	27.49	35.75	31.52	29.07	27.19
FFDNet [33]	-	35.43	31.87	29.51	27.60	36.36	32.55	30.08	28.11	35.82	31.87	29.55	27.82
RIDNet[2]	Fully pre-trained	36.18	32.98	31.09	29.71	36.99	33.41	31.39	29.99	36.28	32.51	30.47	29.11
	$N = 5$	36.26	33.07	31.20	29.84	37.05	33.47	31.46	30.07	36.33	32.56	30.53	29.18
	$N = 10$	36.28	33.10	31.24	29.88	37.07	33.49	31.48	30.09	36.35	32.57	30.54	29.19
	$N = 15$	36.30	33.12	31.26	29.91	37.09	33.50	31.49	30.10	36.35	32.58	30.55	29.20
	$N = 20$	36.31	33.14	31.28	29.93	37.10	33.51	31.50	30.11	36.36	32.59	30.56	29.21
DnCNN [31]	Fully pre-trained	35.85	32.49	30.51	29.07	36.73	33.12	31.08	29.66	36.16	32.35	30.29	28.91
	$N = 5$	35.93	32.60	30.63	29.20	36.78	33.17	31.14	29.72	36.21	32.40	30.34	28.96
	$N = 10$	35.95	32.64	30.68	29.25	36.81	33.20	31.16	29.75	36.22	32.41	30.36	28.99
	$N = 15$	35.97	32.66	30.71	29.29	36.82	33.21	31.18	29.76	36.23	32.43	30.37	29.00
	$N = 20$	35.99	32.68	30.74	29.31	36.83	33.22	31.19	29.78	36.24	32.44	30.38	29.01
RDN [35]	Fully pre-trained	36.27	33.01	31.08	29.65	37.07	33.48	31.44	30.02	36.22	32.43	30.39	29.02
	$N = 5$	36.33	33.11	31.18	29.76	37.12	33.53	31.49	30.08	36.25	32.46	30.43	29.06
	$N = 10$	36.37	33.15	31.23	29.81	37.14	33.55	31.52	30.11	36.27	32.48	30.44	29.08
	$N = 15$	36.39	33.18	31.27	29.85	37.16	33.57	31.53	30.12	36.27	32.49	30.45	29.09
	$N = 20$	36.41	33.20	31.30	29.89	37.17	33.58	31.54	30.14	36.28	32.49	30.46	29.10

Table 5. Quantitative comparison results. State-of-the-art denoising methods are fine-tuned [31,2,35] and compared with BM3D [9] and FFDNet [33]. Our method outperform the baseline and can consistently raise performance as N is increased.

Method	Urban100	DIV2K testset	BSD68
RIDNet [2]	29.71 \rightarrow 29.89	29.99 \rightarrow 30.09	29.11 \rightarrow 29.19
DnCNN [31]	29.07 \rightarrow 29.26	29.66 \rightarrow 29.74	28.91 \rightarrow 28.98
RDN [35]	29.65 \rightarrow 29.85	30.02 \rightarrow 30.12	29.02 \rightarrow 29.09

Table 6. Change of PSNR values before and after fine-tuning ($\sigma = 40$). During the fine-tuning period, noise level σ is not given in Algorithm 1. Our method can fine-tune the network even without knowing the noise level, since noise level σ is not a significant factor with large N as summarized in Table 2.

better results with a small number of updates on various Gaussian noise levels ($\sigma = 10, 20, 30, 40$), and can outperform the pre-trained baseline models with only 5 iterations ($N = 5$). Note that the performance gaps between the baseline (fully pre-trained) and our fine-tuned networks for 5 iterations ($N = 5$) are large particularly when the noise level is high ($\sigma \geq 30$), and we can elevate PSNR values more than 0.2dB on the Urban100 dataset with only 20 iterations ($N = 20$).

Results without knowing noise level In Table 6, we provide denoising results by fine-tuning DnCNN [31], RIDNet [2], and RDN [35]. Input images are corrupted with Gaussian random noise ($\sigma = 40$). In this experiment, we do not let the Algorithm 1 know the noise level σ during updates, and thus we use σ which is randomly generated between 0 and 50 for 20 iterations ($N = 20$). Compared to the results in Table 5 obtained with known noise level, the performance gain is slightly lower in this setting, but still outperforms the baseline network on various testsets consistently. Note that, the noise variance of the latent patch

with M corresponding patches becomes $\frac{1}{M}\sigma_{\theta_0}^2$ if N is large, and does not depend on the original noise level σ .

Run-time With our NVIDIA 2080Ti Graphics card, it takes around 0.99, 2.49, and 2.64 seconds to restore a 1000×600 image with DnCNN, RDN, and RIDNet with 5 updates ($N = 5$).

Visual results In Figure 4, we provide qualitative comparison results. The input images are corrupted with high-level Gaussian noise ($\sigma = 40$), and RIDNet [2] fine-tuned for 20 iterations ($N = 20$) restores the clean images. Our fine-tuned denoiser can produce visually much better results and restores tiny details compared to the fully pre-trained baseline models.

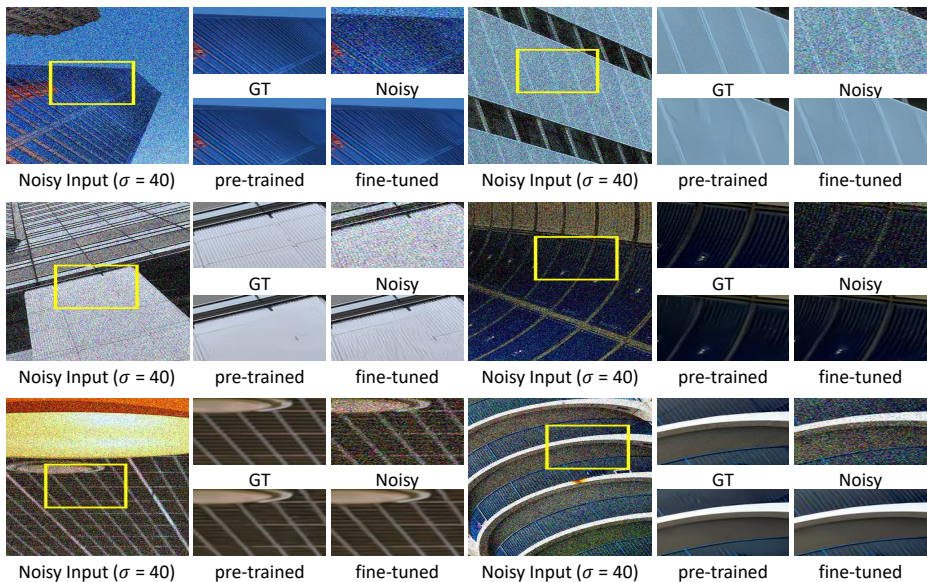


Fig. 4. Visual comparisons. Denoising results by RIDNet [2] before and after fine-tuning ($\sigma = 40$). The *fine-tuned* shows the results obtained after 20 iterations ($N = 20$) with the proposed Algorithm 1.

6 Conclusion

We can improve the performance of the conventional supervision-based denoising methods during test time using the self-similarity property from the given noisy input image with the proposed loss function. Thus, we introduce a new denoising

approach that allows the update of the network parameters from the fully trained version at test time and enhance the image quality significantly by exploiting self-similarity. Our proposed algorithm can be generally applicable to many denoising networks, and we improve the restoration quality significantly without changing the architectures of the state-of-the-art denoising methods. Experimental results demonstrate the superiority of the proposed method.

References

1. Leaderboards. <https://paperswithcode.com/task/image-denoising/latest>, accessed: 2019-11-15
2. Anwar, S., Barnes, N.: Real image denoising with feature attention. In: Proceedings of the IEEE International Conference on Computer Vision (ICCV) (2019)
3. Anwar, S., Huynh, C.P., Porikli, F.: Combined internal and external category-specific image denoising. In: Proceedings of the British Machine Vision Conference (BMVC) (2017)
4. Anwar, S., Porikli, F.M., Huynh, C.P.: Category-specific object image denoising. *IEEE Transactions on Image Processing* **26**, 5506–5518 (2017)
5. Batson, J., Royer, L.: Noise2self: Blind denoising by self-supervision. In: International Conference on Machine Learning (ICML) (2019)
6. Buades, A., Coll, B., Morel, J.: A non-local algorithm for image denoising. In: Proceedings of the IEEE Conference on Computer Vision and Pattern Recognition (CVPR). vol. 2, pp. 60–65 vol. 2 (2005)
7. Buades, A., Coll, B., Morel, J.M.: A non-local algorithm for image denoising. In: Proceedings of the IEEE Conference on Computer Vision and Pattern Recognition (CVPR). pp. 60–65 (2005)
8. Dabov, K., Foi, A., Katkovnik, V., Egiazarian, K.: Image denoising by sparse 3-d transform-domain collaborative filtering. *IEEE Transactions on Image Processing* **16**(8), 2080–2095 (2007)
9. Dabov, K., Foi, A., Katkovnik, V., Egiazarian, K.O.: Image denoising by sparse 3-d transform-domain collaborative filtering. *IEEE Transactions on Image Processing* **16**, 2080–2095 (2007)
10. Dong, W., Zhang, L., Shi, G., Li, X.: Nonlocally centralized sparse representation for image restoration. *IEEE Transactions on Image Processing* **22**(4), 1620–1630 (2013)
11. Dong, W., Li, X., Zhang, L., Shi, G.: Sparsity-based image denoising via dictionary learning and structural clustering. In: Proceedings of the IEEE Conference on Computer Vision and Pattern Recognition (CVPR). pp. 457–464 (2011)
12. Ehret, T., Davy, A., Morel, J.M., Facciolo, G., Arias, P.: Model-blind video denoising via frame-to-frame training. In: Proceedings of the IEEE Conference on Computer Vision and Pattern Recognition (CVPR) (2019)
13. Elad, M., Aharon, M.: Image denoising via sparse and redundant representations over learned dictionaries. *IEEE Transactions on Image Processing* **15**(12), 3736–3745 (2006)
14. Foi, A., Katkovnik, V., Egiazarian, K.: Pointwise shape-adaptive dct for high-quality denoising and deblocking of grayscale and color images. *IEEE Transactions on Image Processing* **16**(5), 1395–1411 (2007)
15. Glasner, D., Bagon, S., Irani, M.: Super-resolution from a single image. In: Proceedings of the IEEE International Conference on Computer Vision (ICCV) (2009)
16. Gu, S., Zhang, L., Zuo, W., Feng, X.: Weighted nuclear norm minimization with application to image denoising. In: Proceedings of the IEEE International Conference on Computer Vision (ICCV). pp. 2862–2869 (2014)
17. Guo, S., Yan, Z., Zhang, K., Zuo, W., Zhang, L.: Toward convolutional blind denoising of real photographs. In: Proceedings of the IEEE Conference on Computer Vision and Pattern Recognition (CVPR) (2018)
18. Huang, J.B., Singh, A., Ahuja, N.: Single image super-resolution from transformed self-exemplars. In: Proceedings of the IEEE Conference on Computer Vision and Pattern Recognition (CVPR) (2015)

19. Krull, A., Buchholz, T.O., Jug, F.: Noise2void-learning denoising from single noisy images. In: Proceedings of the IEEE Conference on Computer Vision and Pattern Recognition (CVPR) (2019)
20. Lefkimmiatis, S.: Non-local color image denoising with convolutional neural networks. In: Proceedings of the IEEE Conference on Computer Vision and Pattern Recognition (CVPR). pp. 5882–5891 (2016)
21. Lehtinen, J., Munkberg, J., Hasselgren, J., Laine, S., Karras, T., Aittala, M., Aila, T.: Noise2Noise: Learning image restoration without clean data. In: International Conference on Machine Learning (ICML). vol. 80, pp. 2965–2974 (2018)
22. Liu, D., Wen, B., Fan, Y., Loy, C.C., Huang, T.S.: Non-local recurrent network for image restoration. In: Advances in Neural Information Processing Systems (NIPS). pp. 1680–1689 (2018)
23. Luo, E., Chan, S.H., Nguyen, T.Q.: Adaptive image denoising by targeted databases. *IEEE Transactions on Image Processing* **24**, 2167–2181 (2015)
24. Mairal, J., Bach, F., Ponce, J., Sapiro, G., Zisserman, A.: Non-local sparse models for image restoration. In: Proceedings of the IEEE International Conference on Computer Vision (ICCV). pp. 2272–2279 (2009)
25. Mairal, J., Elad, M., Sapiro, G.: Sparse representation for color image restoration. *IEEE Transactions on Image Processing* **17**(1), 53–69 (2008)
26. Mairal, J., Bach, F., Ponce, J., Sapiro, G., Zisserman, A.: Non-local sparse models for image restoration. In: Proceedings of the IEEE International Conference on Computer Vision (ICCV). pp. 2272–2279 (2009)
27. Portilla, J., Strela, V., Wainwright, M.J., Simoncelli, E.P.: Image denoising using scale mixtures of gaussians in the wavelet domain. *IEEE Transactions on Image Processing* **12**(11), 1338–1351 (2003)
28. Shocher, A., Cohen, N., Irani, M.: zero-shot super-resolution using deep internal learning. In: Proceedings of the IEEE Conference on Computer Vision and Pattern Recognition (CVPR) (2018)
29. Xie, J., Xu, L., Chen, E.: Image denoising and inpainting with deep neural networks. In: Advances in Neural Information Processing Systems (NIPS). pp. 341–349 (2012)
30. Yue, H., Sun, X., Yu Yang, J., Wu, F.: Image denoising by exploring external and internal correlations. *IEEE Transactions on Image Processing* **24**, 1967–1982 (2015)
31. Zhang, K., Zuo, W., Chen, Y., Meng, D., Zhang, L.: Beyond a gaussian denoiser: Residual learning of deep cnn for image denoising. *IEEE Transactions on Image Processing* **26**, 3142–3155 (2017)
32. Zhang, K., Zuo, W., Gu, S., Zhang, L.: Learning deep cnn denoiser prior for image restoration. In: Proceedings of the IEEE Conference on Computer Vision and Pattern Recognition (CVPR). pp. 2808–2817 (2017)
33. Zhang, K., Zuo, W., Zhang, L.: Ffdnet: Toward a fast and flexible solution for cnn based image denoising. *IEEE Transactions on Image Processing* **27**, 4608–4622 (2018)
34. Zhang, Y., Li, K., Li, K., Zhong, B., Fu, Y.: Residual non-local attention networks for image restoration. In: Proceedings of the International Conference on Learning Representations (ICLR) (2019)
35. Zhang, Y., Tian, Y., Kong, Y., Zhong, B., Fu, Y.: Residual dense network for image restoration. *CoRR* **abs/1812.10477** (2018)
36. Zontak, M., Mosseri, I., Irani, M.: Separating signal from noise using patch recurrence across scales. In: Proceedings of the IEEE Conference on Computer Vision and Pattern Recognition (CVPR) (2013)